

Kinematics of glass to crystal phase transformation in novel multi-component glassy Se–Te–Sn–M (M = Sb, In, Cd) alloys



Namrata Chandel^{a,b}, Neeraj Mehta^{a,*}, Alaa Dahshan^{c,d}

^a Departamento de Física, Universidad Hindú de Banaras, Varanasi, 221005, India

^b Departamento de Física, Sunbeam College Para Mujeres, Varanasi, 221005, India

^c Departamento de Física, Facultad de Ciencias, Universidad King Khalid, P.O. Box 9004, Abha, Saudi Arabia

^d Centro de Investigación de Ciencia de Materiales Avanzados (RCAMS), Universidad King Khalid, P.O. Box 9004, Abha 61413, Saudi Arabia

ARTICLE INFO

Article history:

Received 10 October 2020

Accepted 28 January 2021

Available online 19 February 2021

Keywords:

Chalcogenides

Differential scanning calorimetry

Glass transition temperature

ABSTRACT

The kinetics of the thermally induced glass / crystal phase transformation of chalcogenide glasses plays an important role in determining their candidacy for optical phase change memory applications. The rate of crystallization and the corresponding activation energy are the two crucial kinetic parameters that reflect the durability and quality (i.e., storage properties) of phase change materials. This script deals with metal-induced effects on thermally regulated non-isothermal crystallization in a new glass alloy of Se-Te-Sn using calorimetric measurements. The elements Antimony (Sb), Cadmium (Cd) and Indium (In) have been used as structural modifiers for this purpose. The crystallization and glass transition kinetics of these glass alloys have been investigated by thermal analysis of several kinetic parameters such as the parameter of order n , the maximum crystallization temperature T_c , the crystallization rate K and the consequent activation energy E_c . A DSC is used in non-isothermal mode for the present studies. The values of the activation energy E_c are determined using the data obtained from the displacement of the exothermic peaks of crystallization in non-isothermal DSC plots at various heating rates. The role of the additives Sb, Cd and In in the variation in the rate of crystallization K of and the Avrami index (n) for each glass alloy is also examined. Detailed thermal analysis of the kinetic data confirms the superiority of Cd over the other two additives (In and Sb) for optimization of the kinetic properties of the main SeTeSn glass.

© 2021 SECV. Published by Elsevier España, S.L.U. This is an open access article under the CC BY-NC-ND license (<http://creativecommons.org/licenses/by-nc-nd/4.0/>).

* Corresponding author.

E-mail address: dr.neeraj.mehta@yahoo.co.in (N. Mehta).

<https://doi.org/10.1016/j.bsecv.2021.01.004>

0366-3175/© 2021 SECV. Published by Elsevier España, S.L.U. This is an open access article under the CC BY-NC-ND license (<http://creativecommons.org/licenses/by-nc-nd/4.0/>).

Cinemática de la transformación de fase de vidrio a cristal en nuevas aleaciones vítreas multicomponente Se-Te-Sn-M (M = Sb, In, Cd)

R E S U M E N

Palabras clave:

Calcogenuros

Calorimetría diferencial de barrido

Temperatura de transición del vidrio

La cinética de la transformación de fase vidrio/cristal inducida térmicamente de los vidrios calcogenuros desempeña un papel importante en la determinación de su candidatura para las aplicaciones de memoria óptica de cambio de fase. La tasa de cristalización y la energía de activación correspondiente son los dos parámetros cinéticos cruciales que reflejan la durabilidad y la calidad (es decir, las propiedades de almacenamiento) de los materiales de cambio de fase.

El presente guión trata de los efectos inducidos por metales sobre la cristalización no isotérmica regulada térmicamente en una nueva aleación vítrea de Se-Te-Sn, utilizando mediciones calorimétricas. Los elementos antimonio (Sb), cadmio (Cd) e indio (In) se han empleado como modificadores estructurales para este propósito. La cinética de cristalización y transición vítrea de estas aleaciones de vidrio se ha investigado mediante el análisis térmico de varios parámetros cinéticos como el de orden n , la temperatura máxima de cristalización (T_c), la velocidad de cristalización (K) y la energía de activación consiguiente (E_c). Se usa un DSC en modo no isotérmico para los presentes estudios. Los valores de la energía de activación E_c se determinan utilizando los datos obtenidos del desplazamiento de los picos exotérmicos de cristalización en gráficos de DSC no isotérmicos a diversas velocidades de calentamiento. También se examina el papel de los aditivos Sb, Cd e In en la variación en la K y el índice de Avrami (n) para cada aleación vítrea. El análisis térmico detallado de los datos cinéticos confirma la superioridad del Cd sobre los otros dos aditivos (In y Sb) para la optimización de las propiedades cinéticas del vidrio principal Se-Te-Sn.

© 2021 SECV. Publicado por Elsevier España, S.L.U. Este es un artículo Open Access bajo la licencia CC BY-NC-ND (<http://creativecommons.org/licenses/by-nc-nd/4.0/>).

Introduction

The phase change effects in chalcogenide glasses (ChGs) are attractive for scientific and technological applications in the area of optoelectronics [1–4]. The structural changes that take place in the course of the amorphous-to-crystal transition are an interesting issue in modern physics. In this regard, the devitrification process should be slow to obtain high-class chalcogenide glasses because of their wide applications in the fabrication of optical fibers, waveguides, and optical elements and lenses. On the other hand, it should be fast during the erasing process in phase-change optical recording in CDs and DVDs [2,3]. Thus, the study of crystallization kinetics of newly developed multi-component glasses has become a basic requirement for their use in the expertise behind the device fabrication like phase change optical and electrical memories [4].

The atomic arrangements behind the phase-change mechanism in phase change materials based on ChGs are still uncertain. This is a serious hindrance to their utilization with full competency [5]. Crystallization kinetics plays an important role to help in this direction. A systematic understanding of the crystallization kinetics might also contribute to the breakthrough of novel and future materials. In particular, the awareness of kinematic of crystallization helps us in understanding the character of the concerned mechanisms. Also, it might endow with information about the crystalline framework, forecasts of devitrification behavior under incredible or unique experimental conditions. Moreover, proper knowledge of the mechanism involved in devitrification also reveals the

functioning of specific elements in the molecular arrangements. This allows us the well-planned and efficient tailoring of innovative materials. In literature, various papers on the physical properties of various binary Se-Te and ternary SeTeM glassy semiconducting alloys are available [6–12]. Tripathi and Kumar studied the role of Cd, In, and Sb additives on the photoconductivity of glassy $Se_{80}Te_{20}$ alloy [6]. They observed that photosensitivity decreases after the incorporation of cadmium, indium, and antimony in the parent binary glass. The photosensitivity also decreases quite significantly after the amorphous films of binary $Se_{80}Te_{20}$ alloy and ternary $Se_{80}Te_{10}In_{10}$ and $Se_{80}Te_{10}Sb_{10}$ alloys are crystallized. Nevertheless, the photosensitivity rises after the crystallization of the $Se_{80}Te_{10}Cd_{10}$ alloy. Chandel et al. studied thermally activated a.c. conduction in SeTeM (M=Cd, In, Sb) glasses for lower concentration (0.5 atomic weight percentage) and higher concentration (10 atomic weight percentage) of Cd, In, and Sb [7,8]. They found that the electrical properties are changed significantly for higher concentrations. In various reports [9–12], it was also observed that a phase reversal appears in the increasing/decreasing trend of different physical properties of $Se_{80-x}Te_{20}M_x$ (M=Cd, In, Sb) at 10 atomic weight percentage. Chandel and Mehta [13] also observed that when Cd, In and Sb are incorporated in $Se_{80}Te_{20}$ glass then thermo-mechanical properties are varied significantly after incorporation of Cd, In, and Sb additives. They also found a correlation between Mohs hardness of Cd, In, and Sb and Vickers hardness of $Se_{80}Te_{10}M_{10}$ (M=Cd, In, Sb) alloys [13]. Therefore, we have used Cd, In, and Sb additives for the present studies and choose 10 atomic weight percentage as their concentra-

Hereof, thermal analysis by using differential scanning calorimeter is the most fundamental technique for achieving that level of scientific ability during the thermal characterization of ChGs. Kinetic analysis of glassy materials using the DSC technique involves the thermal analysis of a variety of kinetic properties. To reveal the information about such kinetic properties in ChGs, we deal with the corresponding kinetic temperatures of vitrification and devitrification. Some examples are the kinetic temperatures, the corresponding activation energies, and the pre-exponential factor. We use the combination of these parameters and formalism of the kinetic model (here JMA model) as a tool to check their candidature for potential applications.

The glass-formation region of tin-based binary and ternary chalcogenide glasses is very narrow and corresponds to a small amount of tin in the alloys. Recently, Georgieva et al. [14] reported the effect of amorphous to crystalline phase transformation on both optical and electrical parameters of thin-film samples of Se–Te–Sn. Further, Kaur et al. [15] investigated the kinematics of crystallization on the bulk glassy samples of the $\text{Se}_{80-x}\text{Te}_{20}\text{Sn}_x$ system. Kumar et al. [16] used two different approaches for the alteration of optical characterization of some alloys of Se–Te system by using their amorphous films. In the first approach, they incorporated Sn as a modifier for modifying the optical parameter. In the second approach, they exposed the amorphous thin films by irradiation of swift heavy ions. The role of tin in changing the electrical properties of parent binary $\text{Se}_{85}\text{Te}_{15}$ glass was reported by Sharma et al. [17,18]. Saraswat et al. reported the bandgap studies on amorphous films of the ternary Se–Te–Sn system [19]. The results of surface conductivity measurement on Sn containing Se–Te binary alloys were reported by Solanki et al. [20]. Kinematics of glass transition and crystallization of Sn containing Se–Te binary alloys was reported by Kumar et al. [21,22]. They [21,22] found that the kinetics of glass transition and crystallization of $\text{Se}_{80}\text{Te}_{20}$ glass is affected significantly after the addition of Sn.

The general observation of these studies is that most of the Tin containing ChGs have the drawback of low electronic conductivity, extreme volume expansion, and rigorous accumulation during the cyclic route. These facts appreciably hamper their practical applications. To resolve these issues, the most effective strategy is the incorporation of the foreign element in ternary Se–Te–Sn systems. A lot of fundamental work is already reported in the literature on the crystallization kinetics of the ternary system of Se–Te with Sn as a foreign element. However, the thermal characterization of novel quaternary glasses of this system is not resolved.

In the above thorough literature survey, we have noticed that the effect of foreign elements on a variety of physical and chemical properties in binary and ternary alloys of Selenium rich glasses has been studied by different research groups by altering the concentration but no serious effort has been done to investigate crystallization kinetics in multi-component (ternary and quaternary) alloys by changing the additives in a ternary parent glass for a fixed composition. Currently, a series of papers have been reported in the last decade to understand the outcome of different metallic additives on various physical properties of the Se–Te–Sn system [23–26] after their inclusion and then changing their composition. Sharma et al. [23]

observed that the specific Heat in Multi-component glasses of Se–Te–Sn–Pb is changed appreciably after the addition of lead as the fourth element in the parent Se–Te–Sn system. Sharma and Mehta [24] reported that the incorporation of Pb can also enhance the dielectric relaxation and thermally activated a.c. conduction in the Se–Te–Sn system. Pal et al. [25] studied glass/crystal phase transition in the Se–Te–Sn–Ge system and found that Ge plays a significant role to control the kinematics of glass transition and crystallization of $\text{Se}_{78}\text{Te}_{20}\text{Sn}_2$ glass. Srivastava et al. [26] found that the glass transition temperature decreases slightly with the increase in silver concentration due to the reduction in the cohesive energy of the glass matrix.

Keeping in mind this fact, we have used a different approach in the present work i.e., we have fixed the composition and varied the foreign element. We have executed a systematic experiment for thermal analysis of the crystallization kinetics in Sn containing Se–Te parent alloy before and after the inclusion of Sb, In, Cd additives. Such results are useful to understand the “metal-induced effects” for a fixed concentration (here 10 atomic weight percentage %).

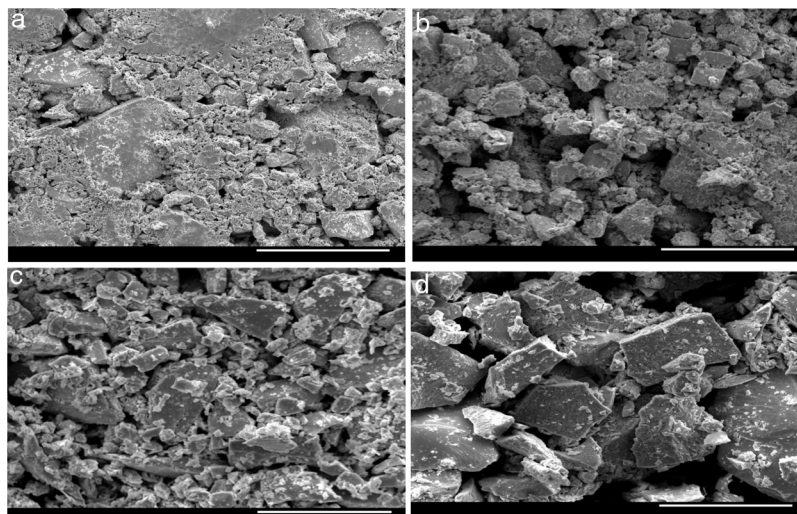
Experimental

The source materials (i.e., Sn containing Se–Te parent alloy and its quaternary alloys having dopants Sb, In, Cd) were synthesized by direct retort of highly pure elemental Se, Te, Sn, Sb, In, Cd. The melt-quench approach was used for this purpose. The atomic weight percentages of elements in each alloy are described in Table 1. Weighing of the desired amounts of the constituent elements was done according to their atomic-weight percentages and after then each sample was sealed in a quartz ampoule under a high vacuum ($\sim 1 \mu\text{-Torr}$). Each sealed ampoule containing the materials was kept inside an organized furnace to raise the temperature to a fixed and high temperature ($> \text{m.p.}$ of the constituents of the ampoule). The holding time in the furnace was 10 h and each ampoule was rotated frequently to inter-mix the constituents. This step is necessary for maintaining the homogeneity of the final product. The tubes were then dipped rapidly in ice water to achieve glasses. The surface morphology of quenched samples was investigated using Scanning Electron Microscope (SEM) (Model: Quanta 200F). Fig. 1 shows the SEM pictures of all samples. From these micro-pictures, it is revealed that there is no sign of any kind of crystal growth. This indicates the glassy character of quenched samples.

For the thermal analysis of each sample, we employed a state of art Differential scanning calorimetry (TA Instruments, Model: Q20 MDSC) to note-down the caloric signs under non-isothermal conditions. About 5–10 mg of the crushed sample was enclosed in an aluminum pan, and then the pan was heated in the DSC cell at different heating rates. The changes in heat flow were measured under an N_2 atmosphere at a constant flow rate ($\sim 40 \text{ mL}$). Each DSC scan, (see Fig. 2) at different heating rates (5, 10, 15, 20 K/min), showed a distinct endothermic and exothermic peak at the glass transition and crystallization temperature T_g and T_c respectively as the indicators of the homogeneousness of the samples. This is a fundamental condition to utilize ChGs as phase-change materials in the optical recording memory. The appearance of

Table 1 – Data for the preparation of glassy Se–Te–Sn and Se–Te–Sn–M (M = Sb, In, Cd) alloys.

System.	Element	Atomic Weight	%	Atomic Weight %	Actual Weight (gm)
SeTeSn	Se	78.96	80	6316.8	3.5684
	Te	127.6	18	2296.8	1.2974
	Sn	118.71	2	237.42	0.1341
SeTeSnCd	Se	78.96	80	6316.8	3.6307
	Te	127.6	8	1020.8	0.5867
	Sn	118.71	2	237.42	0.1365
	Cd	112.41	10	1124	0.6461
SeTeSnIn	Se	78.96	80	6316.8	3.6206
	Te	127.6	8	1020.8	0.5851
	Sn	118.71	2	237.42	0.1361
	In	114.82	10	1148.2	0.6581
SeTeSnSb	Se	78.96	80	6316.8	3.5921
	Te	127.6	8	1020.8	0.5805
	Sn	118.71	2	237.42	0.1350
	Sb	121.75	10	1217.6	0.6924

**Fig. 1 – SEM pictures of glassy (a) Se–Te–Sn, (b) Se–Te–Sn–Cd, (c) Se–Te–Sn–In, (d) Se–Te–Sn–Sb at 100 μm resolution.**

distinct glass transition peaks also confirms the glassy nature of as-prepared samples. Thus, the results of DSC patterns of the present samples are in good agreement with that of SEM images.

Results and discussions

The crystallization temperature has a vital contribution to the understanding of the crystallization of different types of amorphous semiconductors and semiconducting glasses [27–32]. The values of T_c for all the samples at

diverse heating rates are given in Table 2. This table reveals that T_c is increased after the replacements of Te atoms by Sb, Cd and In additives in parent glassy alloy. The increasing sequence of crystallization temperature (T_c) is (Se–Te–Sn) < (Se–Te–Sn–Cd) < (Se–Te–Sn–In) < (Se–Te–Sn–Sb). This rising order can be explained in terms of the rate of crystallization. The rate of crystallization can be expressed by following the Arrhenius equation:

$$K = K_0 \exp\left(-\frac{E_c}{RT}\right) \quad (1)$$

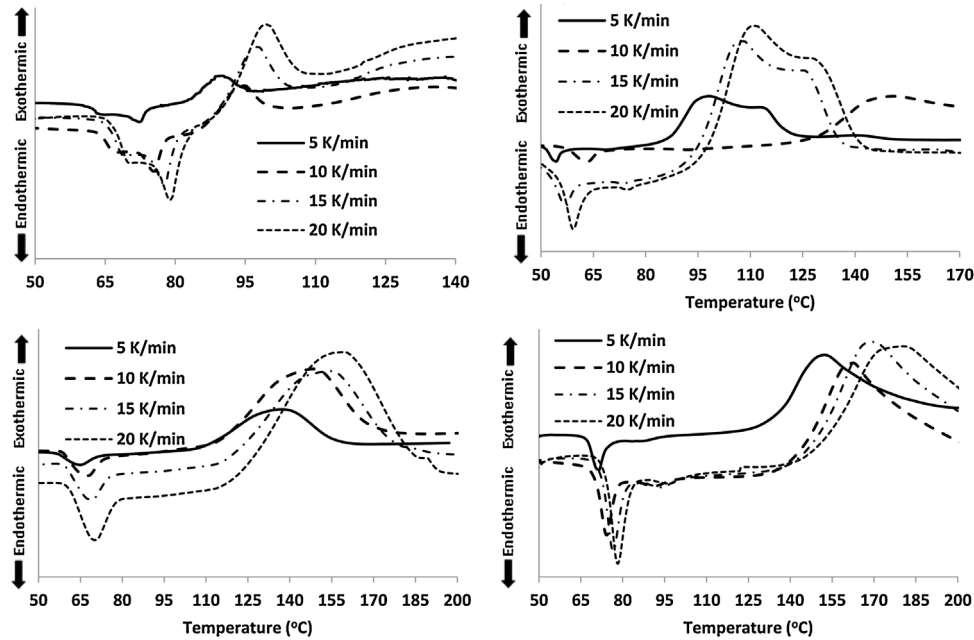


Fig. 2 – DSC scans of glassy (a) Se-Te-Sn, (b) Se-Te-Sn-Cd, (c) Se-Te-Sn-In, (d) Se-Te-Sn-Sb at different heating rates.

Table 2 – Peak crystallization temperature ($T_c/^\circ\text{C}$) and the peak value of the rate of crystallization (K_p/min^{-1}) for glassy Se-Te-Sn and Se-Te-Sn-M ($M = \text{Sb, In, Cd}$) alloys at different heating rates.

Heating rate (β) (K/min)	Se-Te-Sn		SeTeSnCd		SeTeSnIn		SeTeSnSb	
	T_c ($^\circ\text{C}$)	K_p (min^{-1})	T_c ($^\circ\text{C}$)	K_p (min^{-1})	T_c ($^\circ\text{C}$)	K_p (min^{-1})	T_c ($^\circ\text{C}$)	K_p (min^{-1})
5	90.2	0.8	98.2	0.5	137.4	0.3	152.5	0.2
10	94.7	1.5	103.7	1.0	148.9	0.6	162.5	0.5
15	97.4	2.2	107.6	1.5	154.8	0.9	168.9	0.7
20	99.4	2.9	111.1	2.0	159.1	1.1	180.6	0.8

Here, E_c represents the activation energy involved in devitrification. Here R is the universal gas constant while K_0 denotes the pre-factor corresponding to the rate constant.

Gao and Wang [33] developed the following relation using the JMA equation to determine the crystallization reaction rate constant (K_p) is expressed as:

$$K_p = \frac{\beta E_c}{RT_c^2} \quad (2)$$

This parameter provides knowledge about the morphology of crystal growth in glassy alloys. Here, K_p signifies the value of K at temperature T_c corresponding to the crystallization peak for an invariable heating rate. The values of K_p for glassy Se-Te-Sn and Se-Te-Sn-M ($M = \text{Sb, In, Cd}$) alloys are also given in Table 2. One can realize easily that the rising order of K_p in present glasses is just contrary to that of temperature T_c corresponding to the crystallization peak. This indicates that the crystallization of glassy alloys having a lower rate of crystallization starts at a higher temperature.

When we incorporate additives (Sb, In, Cd) in parent Se-Te-Sn, the increasing sequences of three kinetic parameters T_c , $\ln K$, and K_p in quaternary glasses are as follows:

- $(T_c)_{\text{Cd}} < (T_c)_{\text{In}} < (T_c)_{\text{Sb}}$
- $(\ln K)_{\text{Sb}} < (\ln K)_{\text{In}} < (\ln K)_{\text{Cd}}$
- $(K_p)_{\text{Sb}} < (K_p)_{\text{In}} < (K_p)_{\text{Cd}}$.

These increasing sequences of the above three kinetic parameters clearly show that the higher the value of $K(T)$ or K_p , the greater the speed of crystallization and hence lower the crystallization temperature in both glassy systems. Fig. 3 shows the variation of K_p with β for quaternary Se-Te-Sn-M ($M = \text{Sb, In, Cd}$) alloys. From this plot, one can understand that the increasing sequence of K_p is the same in both systems for all heating rates and it is highest in the case of Cadmium containing quaternary glass.

Kissinger [34] proposed that the observed shift in the value of crystallization peaks with heating rate variation can be expressed as in terms of the following correlation between T_c and β :

$$\ln \left(\frac{\beta}{T_c^2} \right) = \left(-\frac{E_c}{RT_c} \right) + \text{Const.} \quad (3)$$

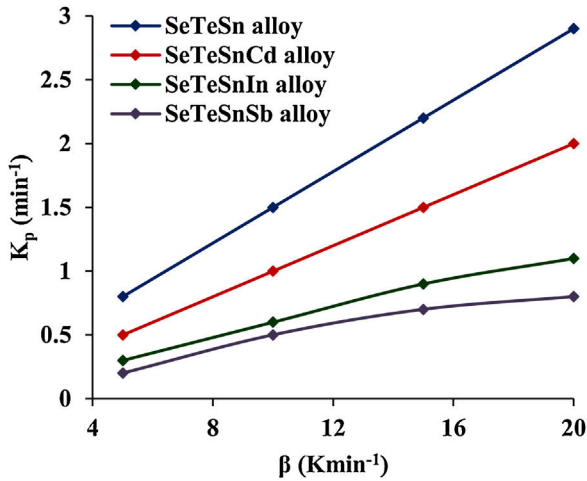


Fig. 3 – Heating rate dependence of K_p for glassy Se–Te–Sn and Se–Te–Sn–M (M = Sb, In, Cd) alloys. Points shown by symbols \blacksquare , \blacktriangle and \bullet stand for Cd, In, and Sb containing glassy alloy respectively.

Similar relations were derived by another researcher [35–37] by using the traditional JMA model which show the following correlations between T_c and β :

$$\ln(\beta) = -\frac{E_c}{RT_c} + \text{const.} \quad (4)$$

$$\ln\left(\frac{\beta}{T_c}\right) = \left(-\frac{E_c}{RT_c}\right) + \ln K_0 \quad (5)$$

The determination of E_c values of different samples is possible by plotting linear curves of $\ln(\beta/T_c^2)$, $\ln(\beta/T_c)$ and $\ln(\beta/T_c^2)$ against $1/T_c$ in Eqs. (3)–(5) respectively.

The plots of $\ln(\beta/T_c)$, $\ln \beta$, and $\ln(\beta/T_c)$ against $1000/T_c$ are shown in Fig. 4. The determination of the E_c values of different samples was done by knowing the values of the slopes of such plots. The values are tabulated in Table 3. From this table, it is clear that the activation energy of crystallization of parent $\text{Se}_{80}\text{Te}_{18}\text{Sn}_2$ glass is reduced after the inclusion of the foreign elements. The reduction in the value of E_c can be revealed by considering the mean atomic volume of the present alloys. It is generally observed in chalcogenide glasses that the crystallization temperature is linked with the progression of the crystal nucleation and their growth and this controls the recrystallization of nearly all glasses. The number of nuclei formed, along with their critical size, from the amorphous phase to the crystalline one, depends on the activation energy. In the present glassy system, the foreign elements have been entered in the glass matrix of parent alloy at cost of Te. The atomic volume ($20.5 \text{ cm}^3/\text{mol}$) of Te is higher than the atomic volumes ($>20.5 \text{ cm}^3/\text{mol}$) of Sb, In, and Cd. Thus, it is reasonable to expect that there is a need for less activation energy to initiate crystallization in an alloy having low atomic volume. In the devitrification of the present parent glass, the larger size of Te atoms causes the rise in the potential barrier and

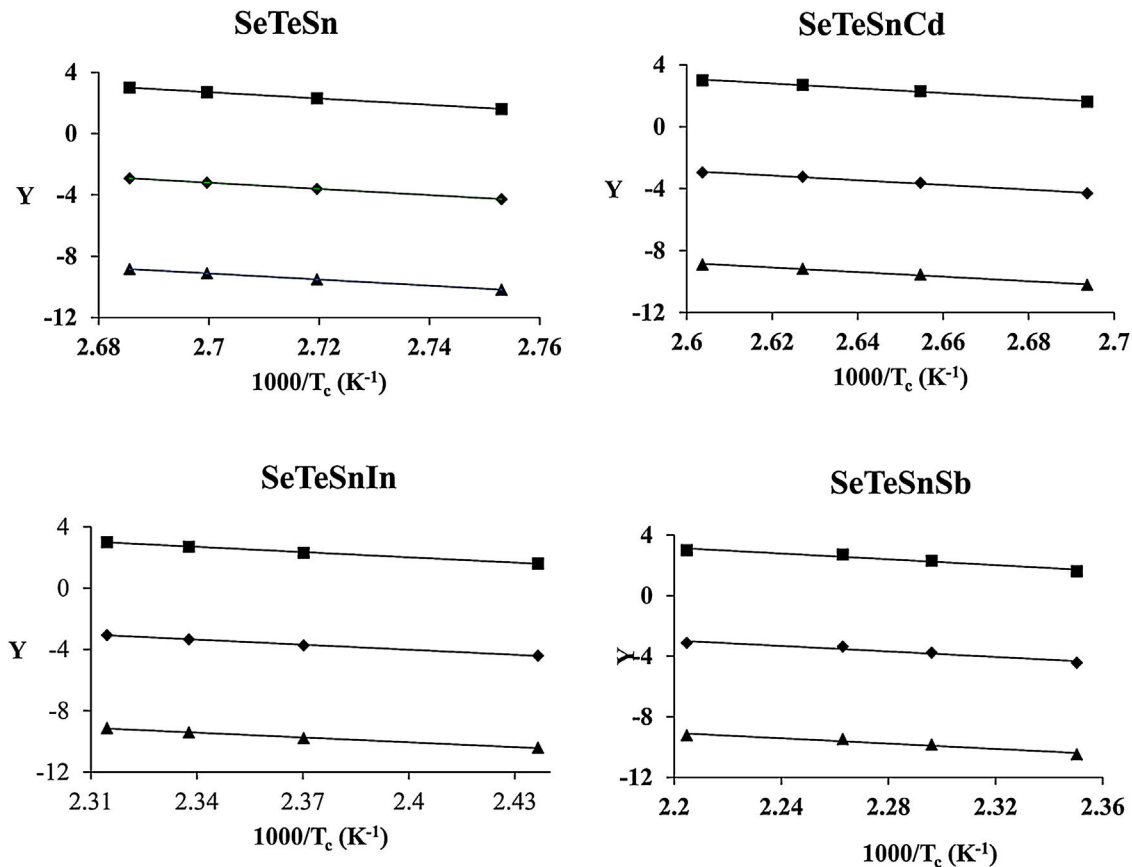


Fig. 4 – Plots of $\ln(\beta)$ vs $10^3/T_c$, $\ln(\beta/T_c)$ vs $10^3/T_c$ and $\ln(\beta/T_c^2)$ vs $10^3/T_c$ for glassy Se–Te–Sn and Se–Te–Sn–M (M = Sb, In, Cd) alloys [\blacktriangle Kissinger method, \blacklozenge Augis–Benett method, and \blacksquare Matusita–Sakka method].

Table 3 – Activation energy of crystallization for glassy Se–Te–Sn and Se–Te–Sn–M (M = Sb, In, Cd) alloys.

Non-isothermal method	E_c (kJ/mol)			
	Se–Te–Sn	SeTeSnCd	SeTeSnIn	SeTeSnSb
Kissinger method	164.6	122.3	87.1	72.6
Augis–Bennett method	167.7	125.5	90.6	76.2
Matusita–Sakka method	170.7	128.6	94.1	79.9
Average value	167.7	125.5	90.6	76.2

Table 4 – Rate constant $\ln K$ (T) for glassy Se–Te–Sn and Se–Te–Sn–M (M = Sb, In, Cd) alloys in the crystallization region at a particular temperature.

Se–Te–Sn		SeTeSnCd		SeTeSnIn		SeTeSnSb	
T (K)	$\ln K$ (min ⁻¹)	T (K)	$\ln K$ (min ⁻¹)	T (K)	$\ln K$ (min ⁻¹)	T (K)	$\ln K$ (min ⁻¹)
361	3.6×10^{46}	361	9.6×10^{33}	413	1.2×10^{21}	413	1.3×10^{17}
366	1.6×10^{46}	366	5.5×10^{33}	423	6.3×10^{20}	423	7.8×10^{16}
371	8.0×10^{45}	371	3.0×10^{33}	433	3.5×10^{20}	433	4.7×10^{16}

delays the diffusion. As a result, in parent glass, the value of E_c is reduced when we substitute foreign elements having atoms of larger radii as compared to replaced atoms of Te. Consequently, a lower energy barrier is required to conquer the diffusion of atoms and corresponding atomic relocation during the devitrification in quaternary glasses [38].

Obtaining the values of the crystallization activation energy and corresponding pre-factor from Eq. (5), we have determined the values of the crystallization rate. Table 4 tabulates the values of $\ln K$ at diverse temperatures lying in the crystallization range for the present samples. This table points out that K is decreased with rising in temperature and its value is highest for glassy SeTeSnCd alloy. Further, we noticed an interesting observation that the increasing order of rate constant $\ln K$ in the present glasses is similar to that of its peak value K_p .

To determine the Avrami index, the following correlation between the crystallization fraction α at a particular temperature and the uniform heating rate β is used [39]:

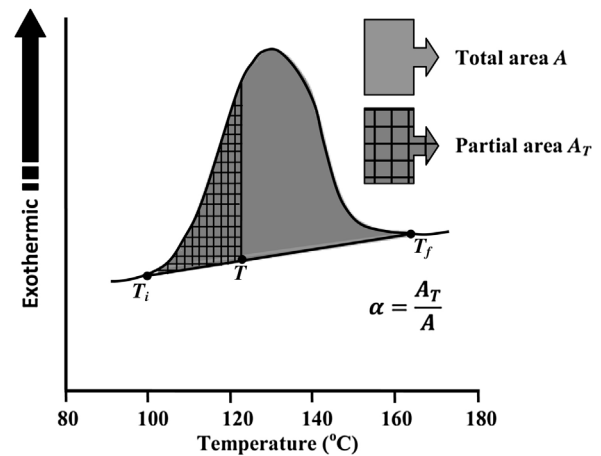
$$\ln[\ln(1 - \alpha)^{-1}] = -n \ln \beta + \text{constant} \quad (6)$$

Avrami index (n) can be evaluated from this equation from the slope of $\ln[\ln(1 - \alpha)^{-1}]$ versus $\ln \beta$ curves plotted at different values of temperature T lying in the crystallization range. At a particular temperature T , the crystallization fraction ' α ' is evaluated from the following relation.

$$\alpha = \frac{A_T}{A} \quad (7)$$

Here, A is the entire area of the crystallization peak having the starting temperature T_i where it starts (i.e. the devitrification is initiated) and the final temperature T_f where it terminates (i.e. the crystallization is completed). The partial area of the exothermic peak corresponding to a temperature T denoted by A_T and it lies between T_i and T (see Fig. 5).

For diverse values of T in the crystallization range, the plots of $\ln[\ln(1 - \alpha)^{-1}]$ versus $\ln \beta$ are shown in Fig. 6 for glassy SeTeSn and SeTeSnM alloys. The values of n are listed in Table 5 for all glassy alloys. The temperature dependence of n is shown in Fig. 7. These plots indicate that there is a

**Fig. 5 – Determination of crystallization fraction ' α ' (degree of conversion) by measuring the area under the exothermic crystallization peak.**

significant reduction in " n " values with the rising temperature. Thus, the increase in the crystallization fraction α with rising temperature in ChGs is a clear indication of this fact [40,41].

We already pointed out that both nucleation and growth play a key role in controlling the re-crystallization. [42]. According to this model, the maximum value that α may attain is unity. The falling tendency in the values of n , therefore, reveals the reduction in the rate of nucleation because of its saturation. Similar results have been observed in numerous second-generation glasses (i.e., ternary systems of ChGs) [25–30].

The mean value of n comes out to be almost 2.5 for ternary SeTeSn alloy and quaternary SeTeSnSb alloy, which shows that the crystallization mechanism in these glasses is bi-dimensional (both two-dimensional and three-dimensional) in these samples. However, the average value of n for quaternary SeTeSnCd and quaternary SeTeSnIn alloys is between 1 and 2. This indicates that the crystal geometry growth is bi-dimensional (both one-dimensional and two-dimensional) in these samples.

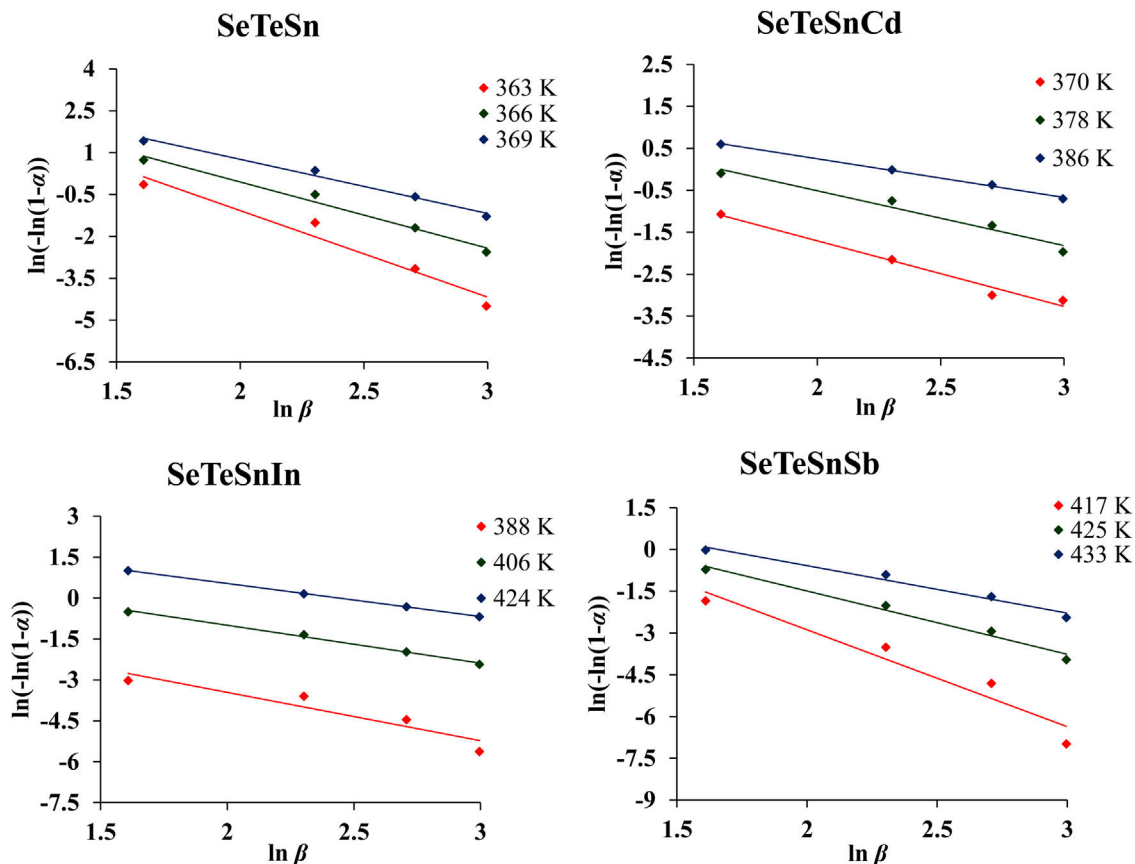


Fig. 6 – Plots of $\ln [-\ln (1 - \alpha)]$ with $\ln \beta$ for a- $\text{Se}_{80}\text{Te}_{18}\text{Sn}_2$ and a- $\text{Se}_{80}\text{Te}_8\text{Sn}_2\text{M}_{10}$ ($\text{M} = \text{Cd}, \text{In}, \text{Sb}$) alloys.

Table 5 – Temperature dependence of Avrami index (n) for glassy Se–Te–Sn and Se–Te–Sn–M ($\text{M} = \text{Sb}, \text{In}, \text{Cd}$) alloys.

SeTeSn		SeTeSnCd		SeTeSnIn		SeTeSnSb	
T (K)	n	T (K)	n	T (K)	n	T (K)	n
363	3.1	370	1.6	388	1.8	417	3.5
366	2.4	378	1.3	406	1.4	425	2.3
369	1.9	386	0.9	424	1.2	433	1.7
Average	2.5		1.3		1.5		2.5

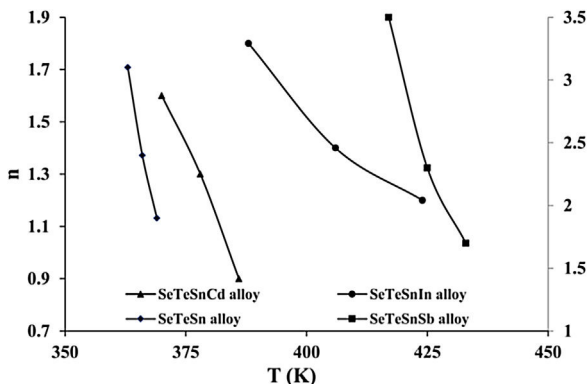


Fig. 7 – Temperature dependence of Avrami index (n). The R.H.S. y-axis stands for the plots of a- $\text{Se}_{80}\text{Te}_{18}\text{Sn}_2$ and a- $\text{Se}_{80}\text{Te}_8\text{Sn}_2\text{Sb}_{10}$ alloys.

Conclusions

Kinematic studies of non-isothermal crystallization on parent SeTeSn glass and elements Antimony (Sb), Cadmium (Cd), and Indium (In) containing quaternary SeTeSnM glasses indicate that values of crystallization temperatures (T_c) are decreased after incorporation of atoms of a foreign element in parent SeTeSn alloy. This is clarified by shifting the peak value of the rate constant of crystallization. The drop off in E_c values after the addition of these additives in the present ternary alloy is explained in terms of reduced mean atomic volume of quaternary alloys. The crystallization mechanism of parent SeTeSn alloy remains unaffected for Sb incorporation. However, it changes from one kind of bi-dimensional (two-dimensional and three-dimensional) growth to another type of bi-dimensional (one-dimensional and two-dimensional) growth after the addition of Cd and In additives. The general observation is that the extreme values for the different kinetic

parameters are obtained in glassy SeTeSnCd alloy. This shows that the insertion of Cd in parent glass SeTeSn affects more efficiently its crystallization mechanism as compared to the other two additives (Sb and In).

Acknowledgments

The author (A. Dahshan) extends his appreciation to the Deanship of Scientific Research at King Khalid University for the financial support through the research groups program under grant number (R.G.P2/113/41). NM is grateful to the Council of Scientific and Industrial Research (CSIR), New Delhi, India for providing financial assistance under a major Project (Scheme no. 03(1453)/19/EMR-II).

REFERENCES

- [1] S.R. Elliott, Chalcogenide phase—change materials: past and future, *Inter. J. Appl. Glass Sci.* 6 (2015) 15–18.
- [2] M. Wuttig, N. Yamada, Phase-change materials for rewriteable data storage, *Nat. Mater.* 6 (2007) 824–832.
- [3] T. Siegrist, P. Merkelbach, M. Wuttig, Phase change materials: challenges on the path to a universal storage device, *Ann. Rev. Cond. Matter Phys.* 3 (2012) 215–237.
- [4] D. Lencer, M. Salinga, M. Wuttig, Design rules for phase—change materials in data storage applications, *Adv. Mater.* 23 (2011) 2030–2058.
- [5] Z. Sun, J. Zhou, R. Ahuja, Structure of phase change materials for data storage, *Phys. Rev. Lett.* 9 (2006) 055507.
- [6] S. Tripathi, A. Kumar, Steady state photoconductivity in amorphous thin films of $\text{Se}_{80-x}\text{Te}_{10}\text{M}_{10}$ ($M = \text{Cd, In, Sb}$), *Thin Films* 189 (1990) 19–25.
- [7] N. Chandel, N. Mehta, A. Kumar, Study of thermally activated a.c. conduction in a- $\text{Se}_{80}\text{Te}_{20}$ and a- $\text{Se}_{80}\text{Te}_{19.5}\text{M}_{0.5}$ ($M = \text{Cd, In, Sb}$) alloys, *Solid State Sci.* 13 (2011) 257–262.
- [8] N. Chandel, N. Mehta, A. Kumar, Investigation of a.c. conductivity measurements in a- $\text{Se}_{80}\text{Te}_{20}$ and a- $\text{Se}_{80}\text{Te}_{10}\text{M}_{10}$ ($M = \text{Cd, In, Sb}$) alloys using correlated barrier hopping model, *Curr. Appl. Phys.* 12 (2012) 405–412.
- [9] A. Singh, J.S.P. Rai, A. Kumar, Calorimetric studies in glassy $\text{Se}_{80-x}\text{Te}_{20}\text{Cd}_x$, *Adv. Mater. Opt. Electron.* 9 (1999) 107–116.
- [10] N. Mehta, A. Kumar, Studies of crystallization kinetics in a- $\text{Se}_{80-x}\text{Te}_{20}\text{Cd}_x$ and a- $\text{Se}_{80-x}\text{Te}_{20}\text{Ge}_x$ alloys using D.C. conductivity measurements, *J. Therm. Anal. Calor.* 83 (2006) 669–673.
- [11] A. Singh, A.K. Nagpal, A. Kumar, Crystallization kinetics in glassy $\text{Se}_{80-x}\text{Te}_{20}\text{Sb}_x$ alloys, *Adv. Mater. Opt. Electron.* 9 (2000) 95–106.
- [12] A. Singh, A.K. Nagpal, A. Kumar, Calorimetric studies in glassy $\text{Se}_{80-x}\text{Te}_{20}\text{Sb}_x$, *Eur. Phys. J. AP* 4 (1998) 323–328.
- [13] N. Chandel, N. Mehta, Study of thermo-mechanical properties of a- $\text{Se}_{80}\text{Te}_{20}$ and a- $\text{Se}_{80}\text{Te}_{10}\text{M}_{10}$ ($M = \text{Cd, In, Sb}$) alloys, *Mater. Lett.* 99 (2013) 35–37.
- [14] I. Georgieva, D. Nesheva, D. Dimitrov, V. Kozhukharov, Influence of crystallization on electrical and optical properties of Te–Se–Sn and Te–Se–Sn–O films, *J. Non-Cryst. Solids* 160 (1993) 105–110.
- [15] G. Kaur, T. Komatsu, R. Thangaraj, Crystallization kinetics of bulk amorphous Se–Te–Sn system, *J. Mater. Sci.* 35 (2000) 903–906.
- [16] S. Kumar, G.B.V.S. Laxmi, M. Husain, M. Zulfequar, Effect of SHI irradiation on Se–Te–Sn thin films, *Eur. Phys. J. Appl. Phys.* 35 (2006) 155–158.
- [17] V. Sharma, A. Thakur, J. Sharma, V. Kumar, S. Gautam, S.K. Tripathi, Electrical properties of a- $\text{Se}_{85-x}\text{Te}_{15}\text{Sn}_x$ thin films, *J. Non-Cryst. Solids* 353 (2007) 1474–1477.
- [18] V. Sharma, J. Ovonic Res, Effect of Sn additive on the electrical properties of Se–Te glassy alloy, *J. Optoelectron. Adv. Mater.* 2 (2006) 35–44.
- [19] V.K. Saraswat, V. Kishore, D.K. Sharma, N.S. Saxena, T.P. Sharma, Bandgap studies on Se–Te–Sn ternary glassy films, *Chalcogenide Lett.* 4 (2007) 61–64.
- [20] D. Solanki, V. Kishore, P.K. Saraswat, A.D. Mittal, S. Gangwar, V.K. Saraswat, Surface conductivity measurement on Se–Te–Sn glasses, *Chalcogenide Lett.* 7 (2010) 263–267.
- [21] H. Kumar, N. Mehta, K. Singh, Calorimetric studies of glass transition phenomenon in glassy $\text{Se}_{80-x}\text{Te}_{20}\text{Sn}_x$ alloys, *Phys. Script.* 80 (2009) 065602.
- [22] H. Kumar, N. Mehta, K. Singh, Calorimetric studies of thermal crystallization in glassy $\text{Se}_{80-x}\text{Te}_{20}\text{Sn}_x$ ($0 \leq x \leq 10$) alloys, *Phys. Script.* 83 (2011) 065602.
- [23] A. Sharma, H. Kumar, N. Mehta, Determination of specific heat in multi-component chalcogenide glasses of Se–Te–Sn–Pb system using modulated differential scanning calorimetry, *Mater. Lett.* 86 (2012) 54–57.
- [24] A. Sharma, N. Mehta, Study of dielectric relaxation and thermally activated A.C. conduction in lead containing multi-component chalcogenide glassy semiconductors (ChGS), *RSC Adv.* 7 (2017) 19085–19097.
- [25] S.K. Pal, N. Chandel, N. Mehta, Synthesis and thermal characterization of novel phase change materials (PCMs) of Se–Te–Sn–Ge (STSG) multi-component system: calorimetric studies of glass/crystal phase transition, *Dalton Trans.* 48 (2019) 4719–4729.
- [26] A. Srivastava, N. Chandel, N. Mehta, Novel explanation for thermal analysis of glass transition, *Mater. Sci. Eng. B* 247 (2019) 114378.
- [27] M.A. El-Oyoun, Crystallization kinetics of the chalcogenide $\text{Bi}_{10}\text{Se}_{90}$ glass, *J. Phy. Chem. Solids* 61 (2000) 1653–1662.
- [28] T. Gill, K.D. Meyer, D.J. Wouters, Amorphous–crystalline phase transitions in chalcogenide materials for memory applications, *Phase Trans.* 81 (2008) 773–790.
- [29] V. Rao, N. Chandel, N. Mehta, D.K. Dwivedi, Effect of antimony on glass transition and thermal stability of $\text{Se}_{78-x}\text{Te}_{18}\text{Sn}_2\text{Sb}_x$ ($x = 0, 2, 4 \text{ \& } 6$ at%) multi component glassy alloys, *J. Therm. Anal. Calorim.* 134 (2018) 915–922.
- [30] K. Samudrala, S.B. Devarasetty, Investigation of Kinetics of crystallization Processes of $\text{S}_{15}\text{–Se}_{85}$, $\text{S}_{15}\text{–Se}_{81}\text{–Cu}_4$ Chalcogenide glasses, *IOP Conf. Ser.: Mater. Sci. Eng.* 149 (2016) 012176.
- [31] H. Kumar, N. Chandel, N. Mehta, Role of Bi incorporation on of glass transition in glassy $\text{Se}_{78}\text{Te}_{20}\text{Sn}_2$ alloy, *Phase Trans.* 89 (2016) 1103–1118.
- [32] D.K. Dwivedi, V. Rao, N. Mehta, N. Chandel, Crystallization kinetics and Avrami index of Sb-doped Se–Te–Sn chalcogenide glasses using iso-conversional techniques, *Phase Trans.* 91 (2018) 490–502.
- [33] Y.Q. Gao, W. Wang, On the activation energy of crystallization in metallic glasses, *J. Non-Cryst. Solids* 81 (1986) 129–134.
- [34] H.E. Kissinger, Reaction kinetics in differential thermal analysis, *Anal. Chem.* 29 (1957) 1702–1706.
- [35] K. Matusita, S. Sakka, Kinetic study of the crystallization of glass by differential scanning calorimetry, *Phys. Chem. Glasses* 20 (1979) 81–84.
- [36] K. Matusita, S. Sakka, Kinetic study on non-isothermal crystallization of glass by thermal analysis, *Bull. Inst. Chem. Res. Kyoto Univ.* 59 (1981) 159–171.
- [37] J. Augis, J. Bennett, Calculation of the Avrami parameters for heterogeneous solid state reactions using a modification of the Kissinger method, *J. Thermal Anal.* 13 (1978) 283–292.
- [38] A. Takeuchi, A. Inoue, Classification of bulk metallic glasses by atomic size difference, heat of mixing and period of

- constituent elements and its application to characterization of the main alloying element, *Mater. Trans.* 46 (2005) 2817–2829.
- [39] K. Matusita, T. Komatsu, R. Yokota, Kinetics of non-isothermal crystallization process and activation energy for crystal growth in amorphous materials, *J. Mater. Sci.* 19 (1984) 291–296.
- [40] K.S. Ranasinghe, C.S. Ray, D.E. Day, A generalized method for determining the crystal nucleation and growth rates in glasses by differential thermal analysis, *J. Mater. Sci.* 37 (2002) 547–555.
- [41] N. Karpukhina, R.G. Hill, R.V. Law, Crystallization in oxide glasses – a tutorial review, *Chem. Soc. Rev.* 43 (2014) 2174–2186.
- [42] E.R. Leite, C. Ribeiro, *Springer Briefs in Materials*, Springer, New York, 2012.